Assimilating satellite microwave radiance measurements over the Antarctic

Craig S. Schwartz and Zhiquan Liu*

NCAR Earth System Laboratory/Mesoscale and Microscale Meteorology Division, Boulder, Colorado, USA

Abstract

As there are few *in situ* observations in and around Antarctica, it is important to assess how assimilating remotely-sensed observations, such as satellite-observed radiances, can fill this observational gap. Thus, a month-long study was conducted over the Antarctic to examine forecast and analysis sensitivity to the assimilation of microwave radiance measurements. Several experiments were configured to quantify the impact of radiance data assimilation (DA) and explore different approaches of radiance bias correction (BC). DA was performed using WRFDA's three-dimensional variational (3DVAR) algorithm, and the analyses initialized 72-hr WRF-ARW forecasts.

The results demonstrate the critical importance of properly bias correcting raw radiance observations. When assimilating radiances using a "cold start" BC technique, forecasts and analyses were degraded compared to those from a parallel experiment that only assimilated conventional (i.e., non-radiance) observations. However, when BC parameters were "spun-up" for several months before the assimilation period, radiance DA yielded forecast and analysis improvements compared to when only conventional observations were assimilated.

1. Introduction

This study examines how assimilating satellite radiances from microwave sensors with the Weather Research and Forecasting Data Assimilation (WRFDA; Barker et al. 2004) three-dimensional variational (3DVAR) algorithm impacts numerical weather prediction (NWP) analyses and forecasts over the Antarctic. In a 3DVAR system, a best-fit "analysis" is calculated considering two sources of initial information: observations at irregularly spaced points and a background (or "first-guess") field, typically taken to be a short-term, gridded model forecast. Associated with the background and observations are their error characteristics. Given the background, observations, and errors, the analysis ($\mathbf{x}$) can be determined by minimizing a scalar cost-function (J) given by

$$J(\mathbf{x}) = \frac{1}{2}(\mathbf{x}-\mathbf{x_b})^{\mathrm{T}}\mathbf{B}^{-1}(\mathbf{x}-\mathbf{x_b}) + \frac{1}{2}(\mathbf{y}-H(\mathbf{x}))^{\mathrm{T}}\mathbf{R}^{-1}(\mathbf{y}-H(\mathbf{x})) \ , \qquad (1)$$

where $\mathbf{x_b}$ denotes the background, $\mathbf{y}$ is the observations, and $\mathbf{B}$ and $\mathbf{R}$ represent the background and observation error covariance matrices, respectively. H is the potentially

*Corresponding author email address: schwartz@ucar.edu

non-linear "observation operator" that interpolates grid-point values to observation locations and transforms model-predicted variables to observed quantities. Eq. (1) is typically linearized about the background field and solved iteratively until the value of **x** is found that minimizes *J*.

Most operational centers currently use variational analysis systems to initialize their NWP models and assimilate microwave radiances[1]. The assimilation of microwave radiances has led to forecast improvements, particularly at intermediate time-ranges (3-7 day forecasts) in global models over areas with few conventional observations[2] (e.g., Caplan et al. 1997; Derber and Wu 1998; Zapotocny et al. 2007, 2008).

However, the impact of radiance data assimilation (DA) within limited-area domains has been less-often studied. Nonetheless, it is important to understand how assimilation of radiances influences regional forecasts, as limited-area and global NWP systems may respond differently to radiance DA due to non-uniform satellite coverage in the former. Moreover, some regional studies have either suggested the forecast impact of radiance assimilation does not persist as long as in a global system (Zapotocny et al. 2005) or found an unclear overall impact (Xu et al. 2009), possibly due to lateral boundary condition (LBC) contamination (Warner et al. 1997).

As there are few *in situ* observations in and around Antarctica, it is important to determine how remotely-sensed observations, such as microwave radiances, can fill this observational gap. Thus, this work examines how radiance DA impacts analyses and forecasts over the Antarctic by performing a month-long sensitivity study. Next, we overview bias correction (BC) of satellite radiances, as this procedure is critical for their successful assimilation. The experimental design is described in section 3. Distributions of the observations are presented in section 4 and results are detailed in section 5 before concluding.

2. Bias correction of satellite radiances

Satellite radiance measurements are prone to systematic errors (i.e., biases) that must be corrected before radiances are assimilated. Although an NWP system may itself be biased, nonetheless, most operational centers measure the observation bias with respect to the NWP system itself. There are different methods of BC, but a popular technique is variational bias correction (VarBC), which performs BC as a part of the analysis, thus considering information from conventional observations and the full background field.

---

[1]Satellites sense radiation at known frequencies, so measured radiances can be converted to brightness temperatures by inverting the Planck function. Most operational centers assimilate brightness temperatures rather than raw radiances, and we do the same.

[2] Herein, "conventional observations" means all observations other than microwave radiance and Global Positioning System radio occultation (GPS-RO) refractivity observations.

VarBC is detailed in Derber and Wu (1998), Dee (2005), and Auligné et al. (2007), but is briefly described here.

In the VarBC approach, a modified observation operator ($\tilde{H}$) is defined that includes corrections to the model-simulated brightness temperatures based on a set of N_p potentially state-dependent predictors (p_i) and their coefficients[3] (β_i):

$$\tilde{H}(\mathbf{x},\beta) = H(\mathbf{x}) + \sum_{i=1}^{N_p} \beta_i p_i(\mathbf{x}). \quad (2)$$

The cost-function [Eq. (1)] is augmented by adding the predictor coefficients to the state ($\mathbf{x}$), thus introducing a parameter background error covariance matrix ($\mathbf{B}_\beta$). $\mathbf{B}_\beta$ determines how much the updated coefficients are weighted toward the background BC coefficients ($\beta_\mathbf{b}$), which are typically values from a previous cycle. A large $\mathbf{B}_\beta$ means the parameter coefficients update quickly when confronted with new observations.

The inclusion of BC coefficients in the state vector and observation operator leads to a modified cost function that is minimized with respect to both $\mathbf{x}$ and $\boldsymbol{\beta}$:

$$J(\mathbf{x},\beta) = \frac{1}{2}(\mathbf{x}-\mathbf{x}_\mathbf{b})^\mathrm{T}\mathbf{B}^{-1}(\mathbf{x}-\mathbf{x}_\mathbf{b}) + \frac{1}{2}(\beta-\beta_\mathbf{b})^\mathrm{T}\mathbf{B}_\beta{}^{-1}(\beta-\beta_\mathbf{b}) + \frac{1}{2}(\mathbf{y}-\tilde{H}(\mathbf{x},\beta))^\mathrm{T}\mathbf{R}^{-1}(\mathbf{y}-\tilde{H}(\mathbf{x},\beta)). \quad (3)$$

Minimizing Eq. (3) updates both the meteorological state variables and BC coefficients simultaneously, thus correcting radiance innovations while preserving the fit to other observations.

BC coefficients can also be updated independently of the analysis using an "offline" method (Auligné et al. 2007). In this approach, the following cost-function is minimized:

$$J(\beta) = \frac{1}{2}(\beta-\beta_\mathbf{b})^\mathrm{T}\mathbf{B}_\beta{}^{-1}(\beta-\beta_\mathbf{b}) + \frac{1}{2}(\mathbf{y}-\tilde{H}(\mathbf{x}_\mathbf{b},\beta))^\mathrm{T}\mathbf{R}^{-1}(\mathbf{y}-\tilde{H}(\mathbf{x}_\mathbf{b},\beta)). \quad (4)$$

This equation is similar to the full VarBC expression [Eq. (3)], except there is no term associated with the background field since $\mathbf{x}_\mathbf{b}$ is assumed to be good. With this assumption, the background is used as the reference from which model-simulated observations are calculated, and the observation vector $\mathbf{y}$ only contains radiance observations. The best-fit to Eq. (4) is achieved solely by updating the vector $\boldsymbol{\beta}$. This method adjusts the radiances toward the background and can result in improved estimates of the BC predictor coefficients.

[3] In WRFDA, there were four state-dependent predictors: 1000-300 hPa thickness, 200-50 hPa thickness, surface skin temperature, and total column precipitable water. In addition, several state-independent predictors based on the satellite scanning angle were used.

3. Experimental design

Several experiments quantified the impact of assimilating microwave radiances over the Antarctic. The experiments differed in terms of the observations they assimilated and/or radiance BC approach. The first experiment (conv+GPS) assimilated conventional and Global Positioning System radio occultation (GPS-RO) refractivity observations (GPS-RO observations were only assimilated between 3- and 18-km). All other experiments assimilated microwave radiances from Advanced Microwave Sounding Unit A and B (AMSU-A, AMSU-B) and Microwave Humidity Sounder (MHS) sensors outfitted on polar orbiting satellites, either instead of or in addition to GPS-RO observations. For example, one experiment (conv+RAD+GPS_spin_up) assimilated conventional, GPS-RO, and radiance observations and used initial BC predictor coefficients that were generated by performing offline analyses every 6-hrs for three months (July-September 2007) using ERA-Interim reanalysis grids as the backgrounds, where the background BC parameters ($\boldsymbol{\beta_b}$) for each cycle were inherited from the previous cycle. A parallel experiment (conv+RAD+GPS) assimilated the same observations but used an initial set of BC coefficients that were *not* spun-up beforehand (hereafter "cold-start BC coefficients"). The last experiment (conv+RAD_spin_up) assimilated just conventional observations and radiances (no GPS-RO data) and also used initial BC coefficients that were spun-up using the offline method. The experimental configurations are summarized in Table 1 and the satellites that were used for radiance DA are listed in Table 2.

Each experiment produced a new analysis every 12 hours beginning 1200 UTC 01 October and ending 1200 UTC 31 October 2007. A 72-hr Advanced Research WRF (ARW; Skamarock et al. 2008) model forecast was initialized from each analysis. The backgrounds for each analysis were 6-hr ARW forecasts initialized at either 0600 or 1800 UTC. In turn, these ARW forecasts were initialized from GFS analyses, and thus, these experiments did not employ cyclic DA in the traditional sense, where the previous analysis cycle's forecast serves as the background ($\mathbf{x_b}$) for the current analysis. However, all experiments that assimilated radiances cycled the predictor coefficients—that is, $\boldsymbol{\beta}$ was updated each analysis with the full VarBC algorithm [(Eq. (3)] using the previous cycle's coefficients as the background (β_b).

Experiment name	Radiances assimilated?	GPS-RO obs assimilated?	Initially spun-up bias-correction coefficients?
conv+GPS	NO	YES	N/A
conv+RAD_spin_up	YES	NO	YES
conv+RAD+GPS_spin_up	YES	YES	YES
conv+RAD+GPS	YES	YES	NO

Table 1. Summary of which experiments assimilated GPS-RO and radiance observations, and specification of the initial BC coefficients.

Satellite	Sensors	Channels
NOAA-15	AMSU-A	5-9

NOAA-16	AMSU-A	5-8
NOAA-17	AMSU-B	3,5
NOAA-18	AMSU-A,MHS	AMSU-A: 5-8; MHS: 3-5
METOP-2	AMSU-A, MHS	AMSU-A: 5,6,8,9; MHS: 3-5

Table 2. Satellites, sensors, and channels that were assimilated.

Aside from assimilating different observations and varying the initial values of the BC coefficients, the experiments were otherwise configured identically, thus permitting a clear assessment of the impact of radiance DA. For example, all experiments were integrated over the same computational domain (Fig. 1). Horizontal grid spacing was 45-km. There were 44 vertical levels and the model top was 10 hPa. Observations within 1.5 hours of the analysis times were assimilated. Radiances were thinned on a 90-km mesh grid and assimilated for non-precipitating pixels only. The Community Radiative Transfer Model (CRTM) was used to calculate model-simulated brightness temperatures. NCEP's Global Forecasting System (GFS) provided LBCs.

4. Observation coverage

DA over the Antarctic is challenging due to few *in situ* observations in the region. Fig. 2 shows a representative snapshot of non-radiance observations available for assimilation over the computational domain. There were a handful of soundings (Fig. 2b) and a fair amount of surface observations (Fig. 2d) taken over the Antarctic continent. But, aside from a few GPS-RO profiles (Fig. 2a), there were virtually no upper-air or surface observations over the sea (Fig. 2c).

Fortunately, satellite coverage over the domain was very good (Fig. 3) and copious radiance observations were assimilated every cycle (Fig. 4). The experiment that used initially spun-up BC coefficients assimilated more radiances each analysis than the experiment using cold-start predictor coefficients. As the background fields were constant for all experiments, the different number of assimilated radiances was entirely due to better estimates of the BC coefficients generated during an offline spin-up, which led to smaller innovations and fewer rejections.

5. Results

As radiance DA is designed to generally make small corrections to the first-guess, it was difficult to discern visual differences among the experiments regarding individual forecasts. Thus, we focus on statistics aggregated over all initializations. Additionally, since there were few sounding sites against which to perform verification, analyses and forecasts were compared to ERA-interim reanalyses interpolated onto the computational domain and considered as "truth." We examine DA impact to the analyses before evaluating forecast accuracy.

a. Analysis accuracy

At the analysis time, domain-wide aggregate root-mean-square-errors (RMSEs; Fig. 5) reveal substantial differences between the experiments. When initial cold-start BC coefficients were used, the analyses were degraded, especially for low- and upper-level wind (Fig. 5a,d,f), but also for low- and mid-level temperature (Fig. 5b). But, above ~150 hPa, the addition of radiances—even without initially spun-up BC coefficients—improved analyses of geopotential height and temperature (Fig. 5b,e).

On average, the best analyses occurred when radiances were assimilated using initially spun-up BC coefficients, either with or without also assimilating GPS-RO data. Temperature analyses below ~850 hPa and wind analyses between ~500-250 hPa were improved with radiance DA. Height analyses were improved above 300 hPa. Moisture analyses (Fig. 5c) were not sensitive to assimilating radiances.

The spatial characteristics of mean aggregate analysis increments of 500 hPa temperature also demonstrate the impact of radiance DA. Without assimilating radiances (Fig. 6a) large increments were generated over Antarctica and the ocean on the western-hemispheric side of the continent. However, with radiance DA (Fig. 6b) the increments were much smaller. These different increment structures were also reflected in the spatial distribution of 500 hPa temperature average RMSE at the initial time (again compared ERA-Interim analyses). Although the aggregate RMSE (Fig. 5) showed little difference between the two experiments at this level, examining a map of the errors reveals large differences (Fig 7). Radiance DA (Fig. 7b) led to much lower RMSEs over the sea, particularly over the region where the analysis increments were smaller (c/f Fig. 6). Over the continent, assimilating radiances led to larger RMSEs in some areas but lower RMSEs in others.

There were also differences in the initial wind field. As microwave radiance measurements are not impacted by wind, differences at the analysis time among the experiments arise due to multivariate background error correlations between the mass and velocity fields. Aggregate RMSEs for 500 hPa wind components (Fig. 8) show that the inclusion of radiances yielded lower RMSEs over the ocean, particularly for the meridional wind component (Fig. 8c,d) but also the zonal wind (Fig. 8a,b). Compared to the RMSEs over the sea, RMSEs were lower over Australia and the eastern side of Antarctica where several soundings were launched (see Fig. 2b), underscoring the value of soundings to DA and NWP systems.

Overall, when BC coefficients were spun-up, radiance DA produced better analyses over the Antarctica, and no systematic degradation was evident, except for a small layer (150-50 hPa) in the wind fields. Otherwise, low-level temperature, mid-level wind, and upper-level height were improved by assimilating radiances.

b. Forecast accuracy

The two experiments that assimilated radiances using initially spun-up BC coefficients yielded improved 12-hr wind forecasts between ~250-500 hPa compared to when radiances were not assimilated or cold-start BC coefficients were used (Fig. 9a,d,f). Additionally, 12-hr temperature (height) forecasts above ~150 hPa (~100-hPa) were also improved by radiance DA (Fig. 9b,e). A slight improvement of 12-hr moisture forecasts below 925 hPa was also noted in the experiments assimilating radiances with spun-up BC coefficients (Fig. 9c). When the initial BC coefficients were not spun-up, forecasts of wind and low-level temperature and moisture were degraded. Again, although the domain-wide statistics revealed no major differences, a map of the RMSE of 12-hr 500 hPa temperature forecasts (Fig. 10) depicts that RMSEs over the sea were substantially reduced when radiances were assimilated with initially spun-up coefficients.

For 24-hr forecasts (Fig. 11), the experiment assimilating radiances with cold-start coefficients produced the worst forecasts of wind and low-level moisture. Wind forecasts were improved in a small mid-level layer (Fig. 11a,d,f) when radiances were assimilated with spun-up coefficients. This improvement was also evident in 48-hr wind forecasts between 300-400 hPa (Fig. 12). Otherwise, by 48-hrs, there were no differences among the four experiments.

6. Discussion and conclusion

A series of experiments were conducted to determine the impact of microwave radiance DA over the Antarctic. 3DVAR analyses were performed every 12 hours at 0000 and 1200 UTC each day in October 2007 using non-cyclic 6-hr ARW forecasts initialized at either 0600 or 1800 UTC as background fields. Each 3DVAR analysis initialized a 72-hr ARW forecast.

The experimental configurations permitted a clean isolation of the impact of radiance DA. On average, when radiance BC coefficients were initialized with values derived from three months of spin-up, the addition of radiances led to better analyses and 12-hr forecasts of mid-level wind, upper-level height, and low- and upper-level temperature. In particular, 500 hPa analyses and 12-hr forecasts of temperature were substantially improved over the ocean. Once the forecasts integrated to 24 and 48 hrs, there was little difference between the experiments, as model error growth and LBC contamination masked any differences. There was little difference between the experiment that assimilated conventional observations, radiances, and GPS-RO observations and the one that assimilated just conventional observations and radiances, suggesting that over this domain radiances were a more important data source.

When the BC coefficients were not initially spun-up, analyses and 12-hr forecasts were degraded for nearly all meteorological variables. Clearly, it is imperative that regional DA systems employ cyclic BC coefficients. Additionally, it is advisable to spin-up the predictor coefficients using an offline method for at least a month before assimilating radiances. Failure to do so may result in degraded analyses and the adverse impact can be carried through to short-range forecasts.

We are quite encouraged to see a positive impact from radiance DA using non-cyclic initial conditions. In general, we would expect parallel cyclic experiments to yield more differences among themselves due to the impact of data accumulation throughout the cycles. Future work will address cyclic DA methods to determine whether additional gains from radiance DA can be realized.

Acknowledgements

NCAR is sponsored by the National Science Foundation. This work was supported by NSF contract ANT-0839068.

References

Auligné T., A. P. McNally, and D. P. Dee, 2007: Adaptive bias correction for satellite data in a numerical weather prediction system. *Quart. J. Roy. Meteor. Soc.*, **133,** 631–642.

Barker, D. M., W. Huang, Y-R. Guo, A. Bourgeois, and X. N. Xio, 2004: A three-dimensional variational data assimilation system for MM5: Implementation and initial results. *Mon. Wea. Rev.*, **132,** 897–914.

Caplan, P., J. Derber, W. Gemmill, S. Y. Hong, H. L. Pan, and D. Parish, 1997: Changes to the 1995 NCEP operational medium-range forecast model analysis–forecast system. *Wea. Forecasting*, **12,** 581–594.

Dee, D. P., 2005: Bias and data assimilation. *Quart . J. Roy. Meteor. Soc.*, **131**, 3323–3343.

Derber, J. C. and W-S. Wu, 1998: The use of TOVS cloud-cleared radiances in the NCEP SSI analysis system. *Mon. Wea. Rev.*, **126,** 2287–2299.

Skamarock, W. C., J. B. Klemp, J. Dudhia, D. O. Gill, D. M. Barker, M. G. Duda, X-Y. Huang, W. Wang, and J. G. Powers, 2008: A description of the Advanced Research WRF version 3. NCAR Tech Note NCAR/TN-475+STR, 113 pp. [Available from UCAR Communications, P. O. Box 3000, Boulder, CO 80307.]

Warner, T. T., R. A. Peterson, and R. E. Treadon, 1997: A tutorial on lateral boundary conditions as a basic and potentially serious limitation to regional numerical weather prediction. *Bull. Amer. Meteor. Soc.*, **78,** 2599–2617.

Xu, J, S. Rugg, L. Byerle, and Z. Liu, 2009: Weather forecasts by the WRF-ARW model with the GSI data assimilation system in the complex terrain areas of Southwest Asia. *Wea. Forecasting*, **24,** 987-1008.

Zapotocny, T. H., W. P. Menzel, J. A. Jung, and J. P. Nelson III, 2005: A four-season

impact study of rawinsonde, GOES, and POES data in the Eta Data Assimilation System. Part II: Contribution of the components. *Wea. Forecasting*, **20,** 178–198.

Zapotocny, T. H., J. A. Jung, J. F. Le Marshall, and R. E. Treadon, 2007: A two-season impact study of satellite and in situ data in the NCEP Global Data Assimilation System. *Wea. Forecasting*, **22,** 887–909.

Zapotocny, T. H., J. A. Jung, J. F. Le Marshall, and R. E. Treadon, 2008: A two-season impact study of four satellite data types and rawinsonde data in the NCEP

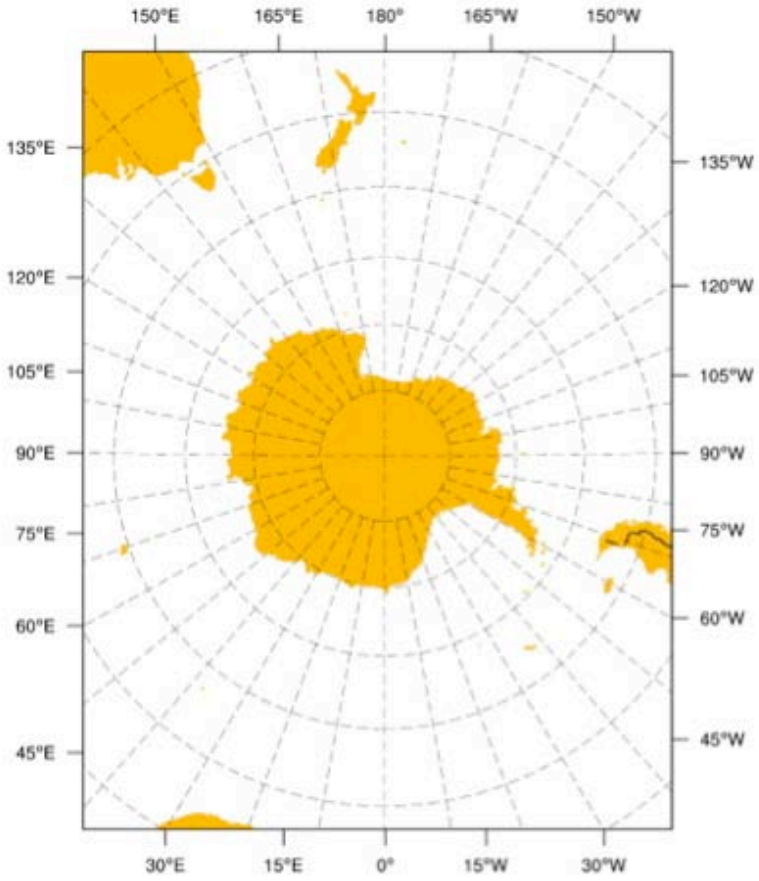

Fig. 1. Computational domain used for all experiments.

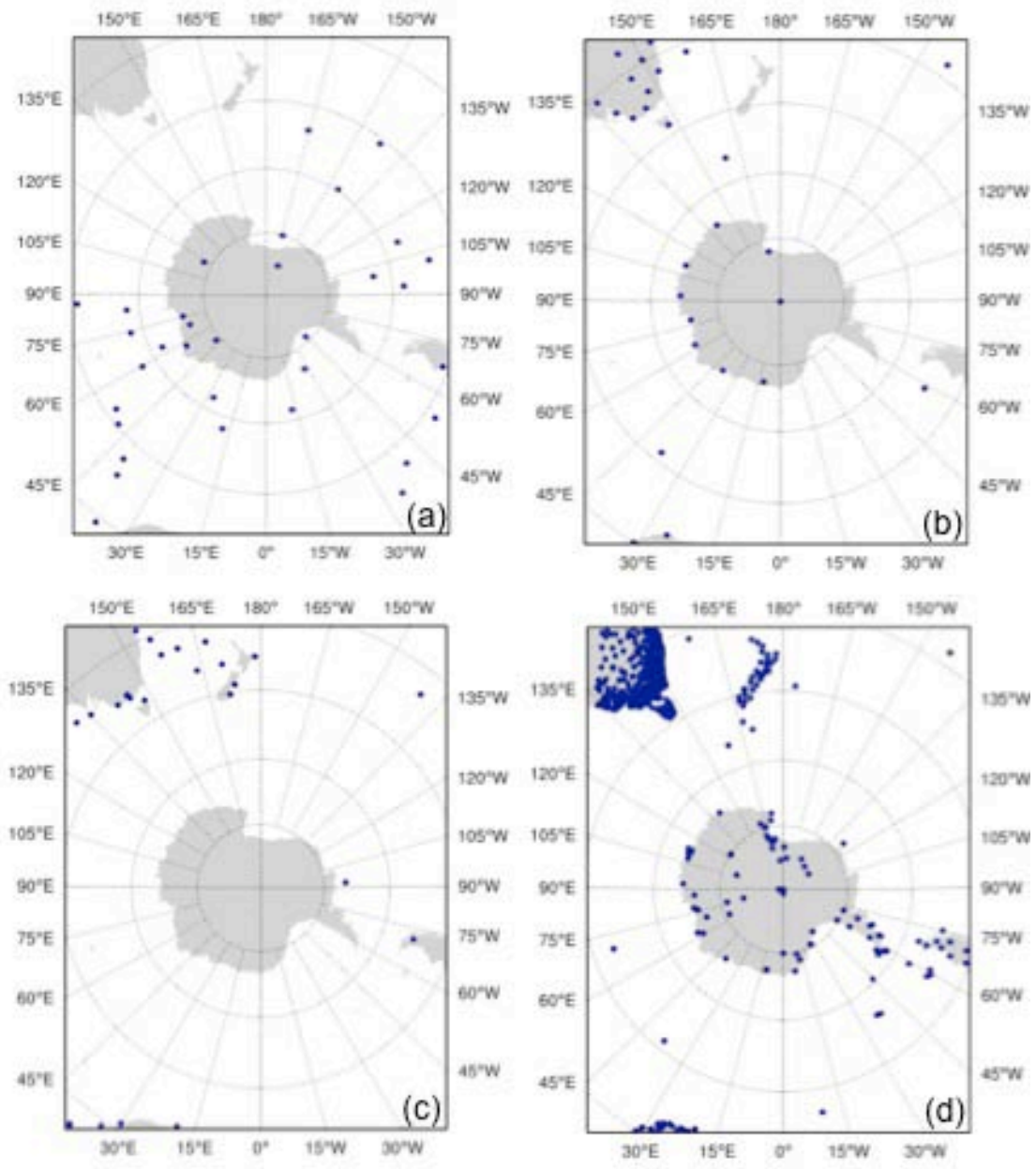

Fig. 2. Snapshot of (a) GPS-RO, (b) sounding, (c) ship, and (d) synop observations available for assimilation for the 0000 UTC 02 October analysis.

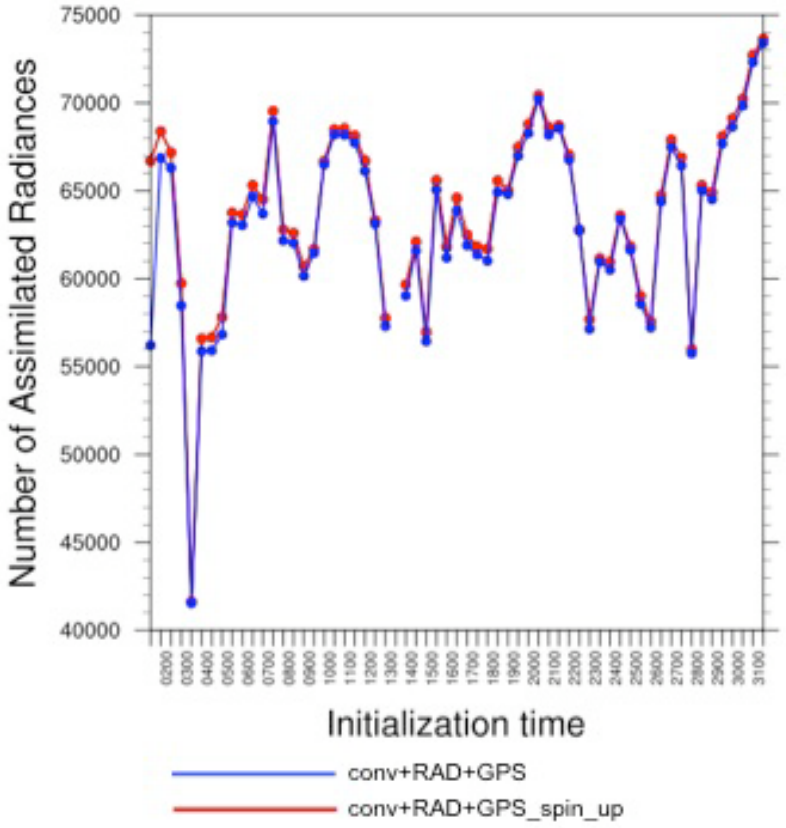

Fig. 3. Number of radiances actually assimilated each analysis for the experiments using initially spun-up BC coefficients (conv+RAD+GPS_spin_up; red line) and cold-start BC coefficients (conv+RAD+GPS; blue line)

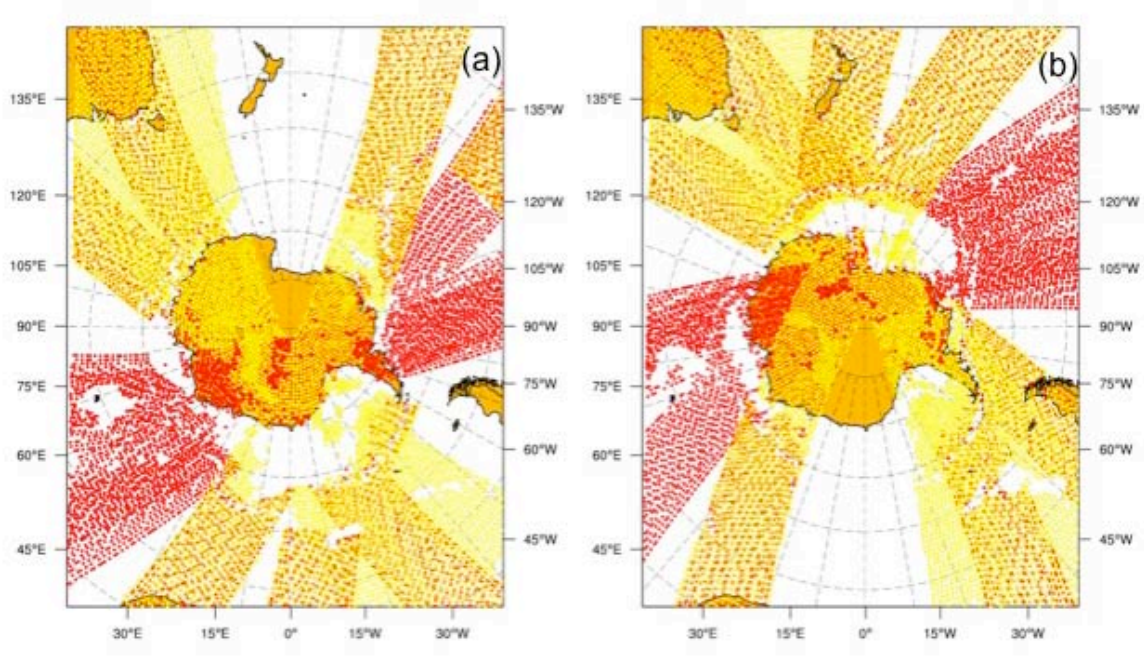

Fig. 4. Spatial distribution of radiances that were actually assimilated during the (a) 0000 UTC 05 October and (b) 1200 UTC October analyses. Red dots represent observations from AMSU-A sensors and yellow dots observations from AMSU-B or MHS sensors.

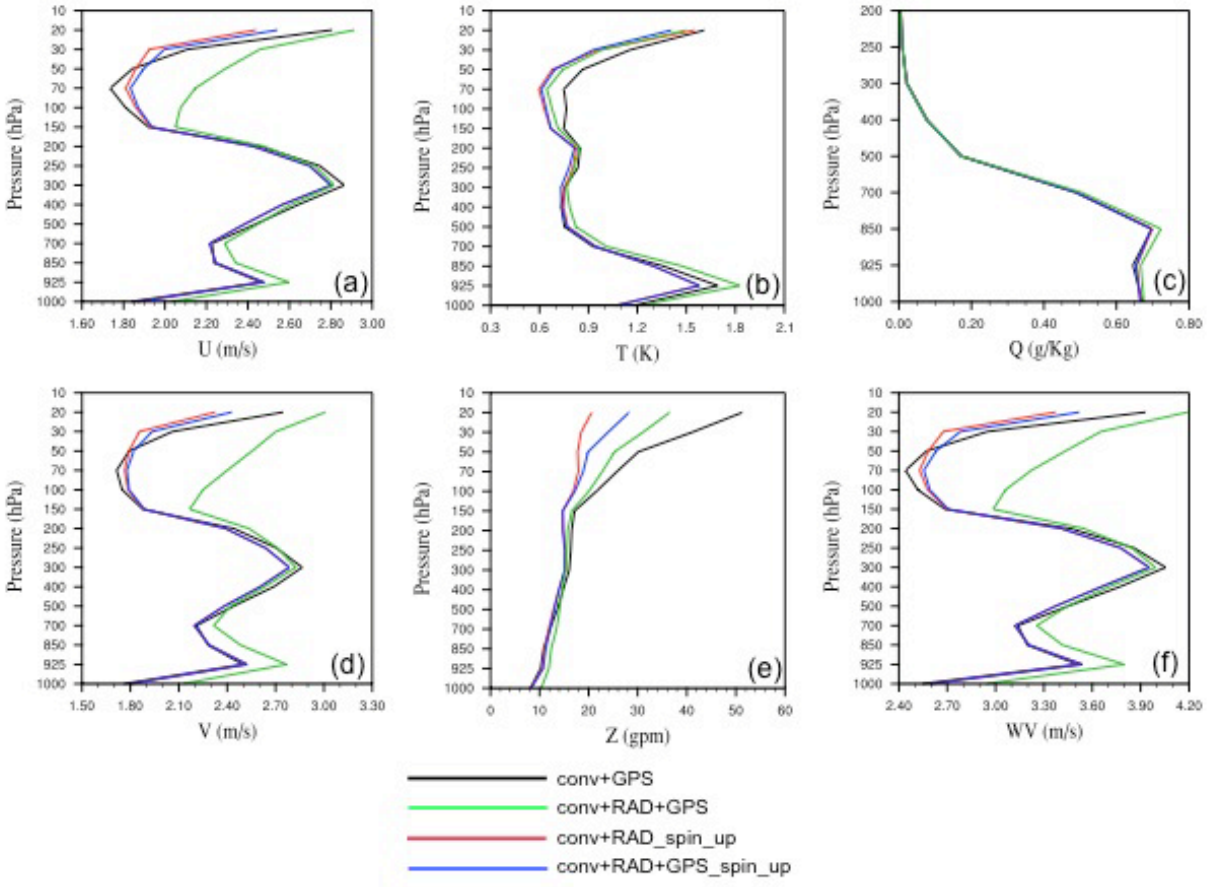

Fig. 5. Domain-wide RMSE aggregated over all initializations for the analysis time. Meteorological variables and their units are specified on the figures: U—zonal wind component; V—meridional wind component; T—temperature; Q—specific humidity; Z—geopotential height; WV—wind vector. The wind vector RMSE is calculated as $RMSE_{WV} = \sqrt{(u_m - u_{ref})^2 + (v_m - v_{ref})^2}$, where the subscripts "m" and "ref" refer to the model and reference fields (i.e., ERA-Interim reanalyses), respectively.

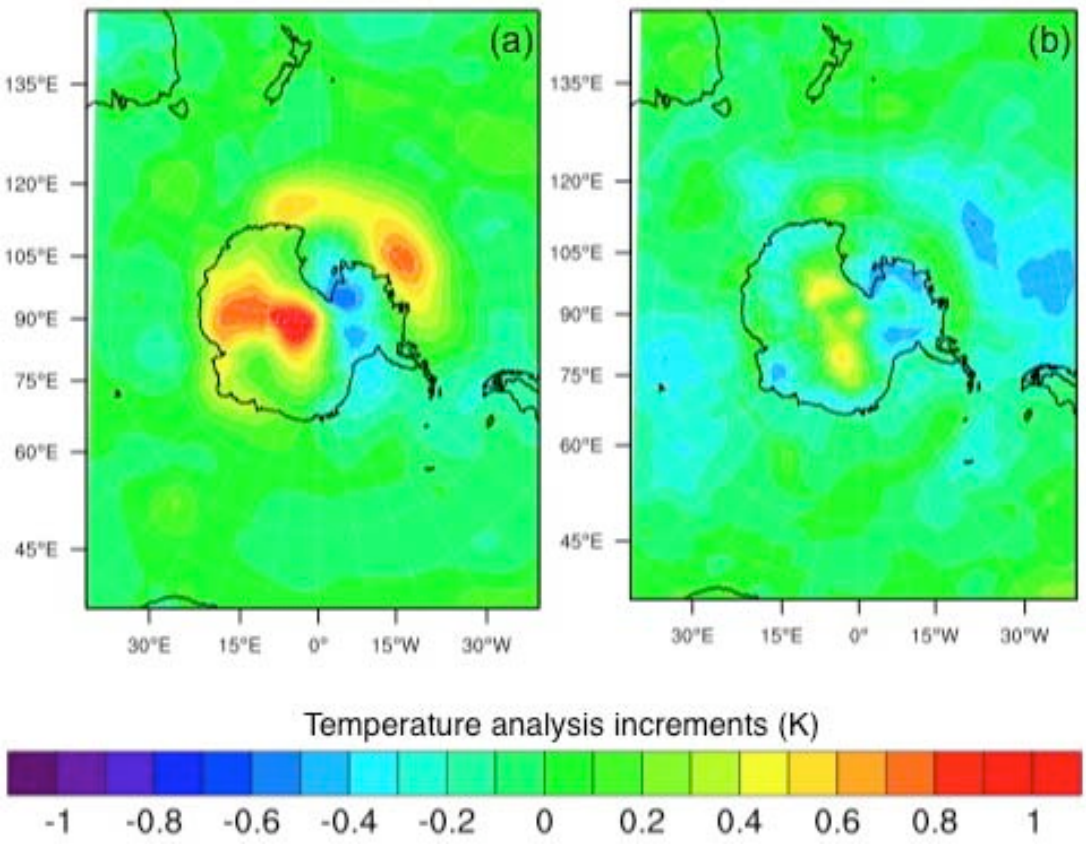

Fig. 6. Aggregate analysis increments of 500 hPa temperature for (a) the experiment that only assimilated GPS-RO and conventional observations (conv+GPS) and (b) the experiment that assimilated radiances in addition to GPS-RO and conventional observations (conv+RAD+GPS_spin_up)

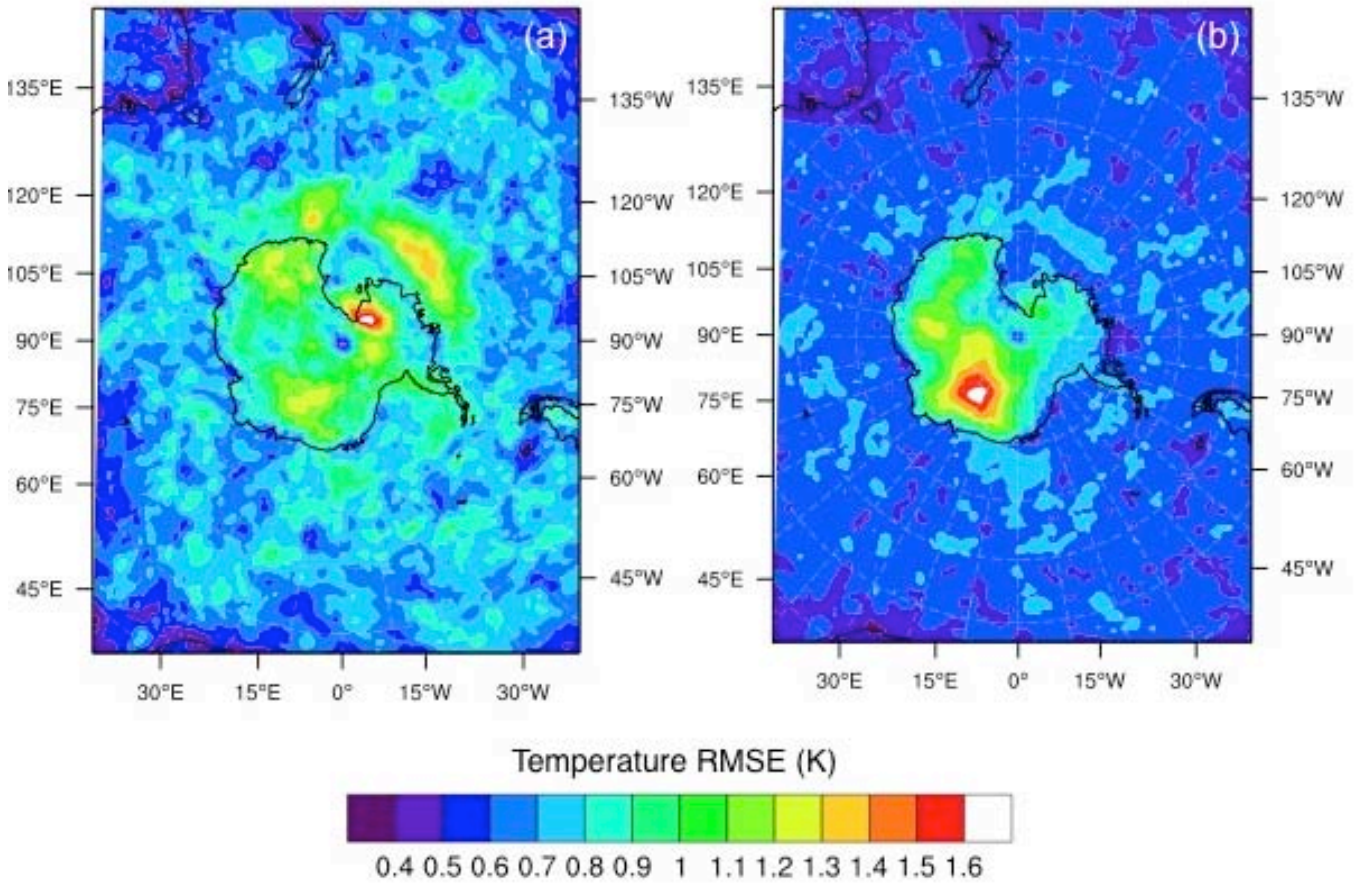

Fig. 7. As in Fig. 6, except the aggregate RMSE at the initial time of 500 hPa temperature is plotted.

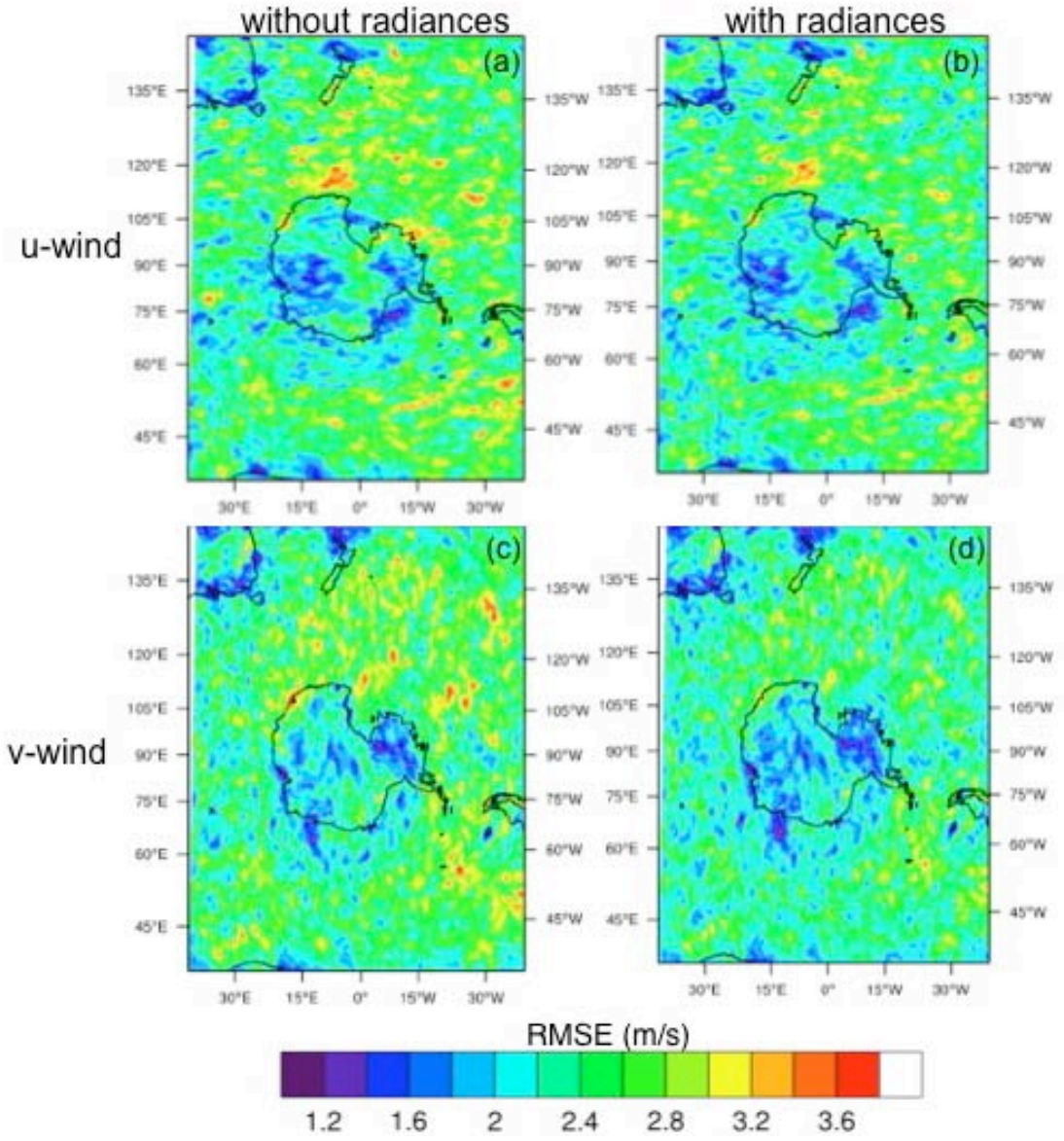

Fig. 8. Aggregate analysis increments of 500 hPa (a)-(b) zonal wind and (c)-(d) meridional wind the experiment that assimilated radiances in addition to GPS-RO and conventional observations (conv+RAD+GPS_spin_up; right column) and (b) the experiment that only assimilated GPS-RO and conventional observations (conv+GPS; left column).

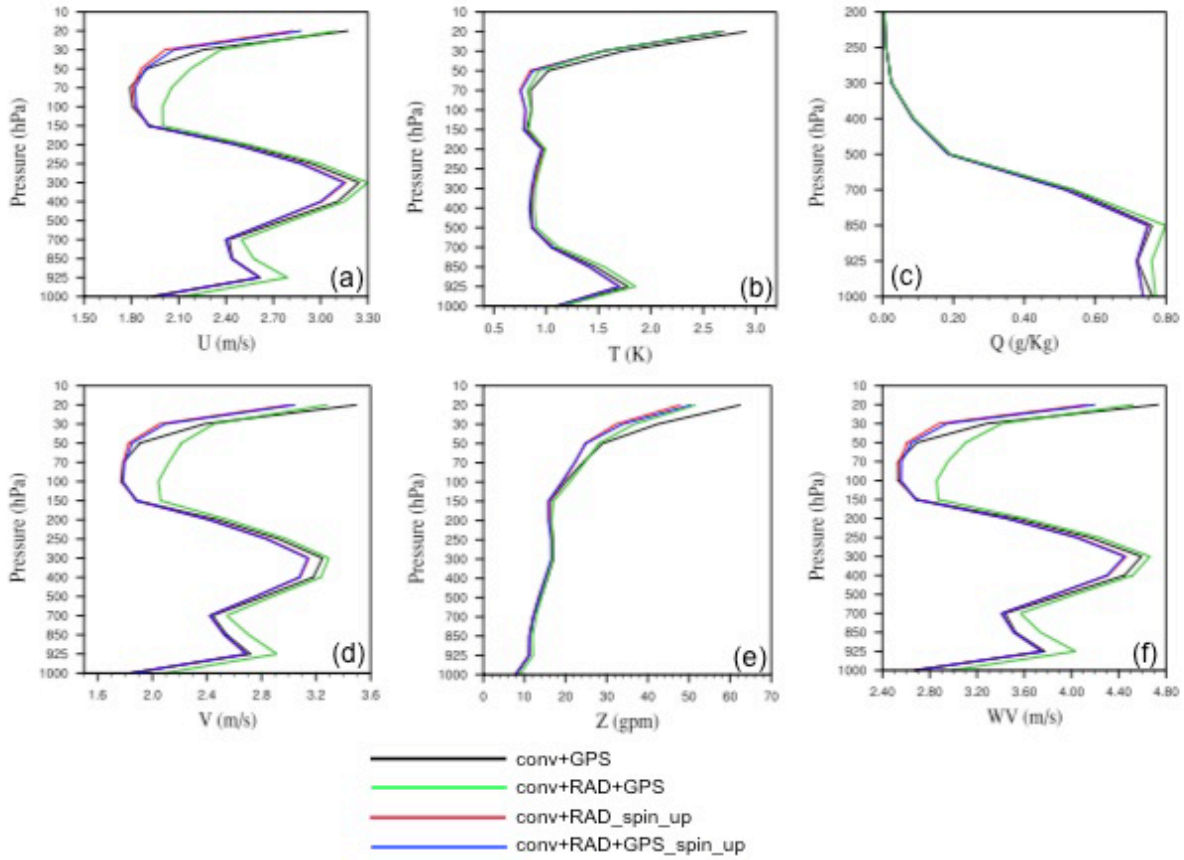

Fig. 9. As in Fig. 5, except the aggregate RMSE of 12-hr forecasts is plotted.

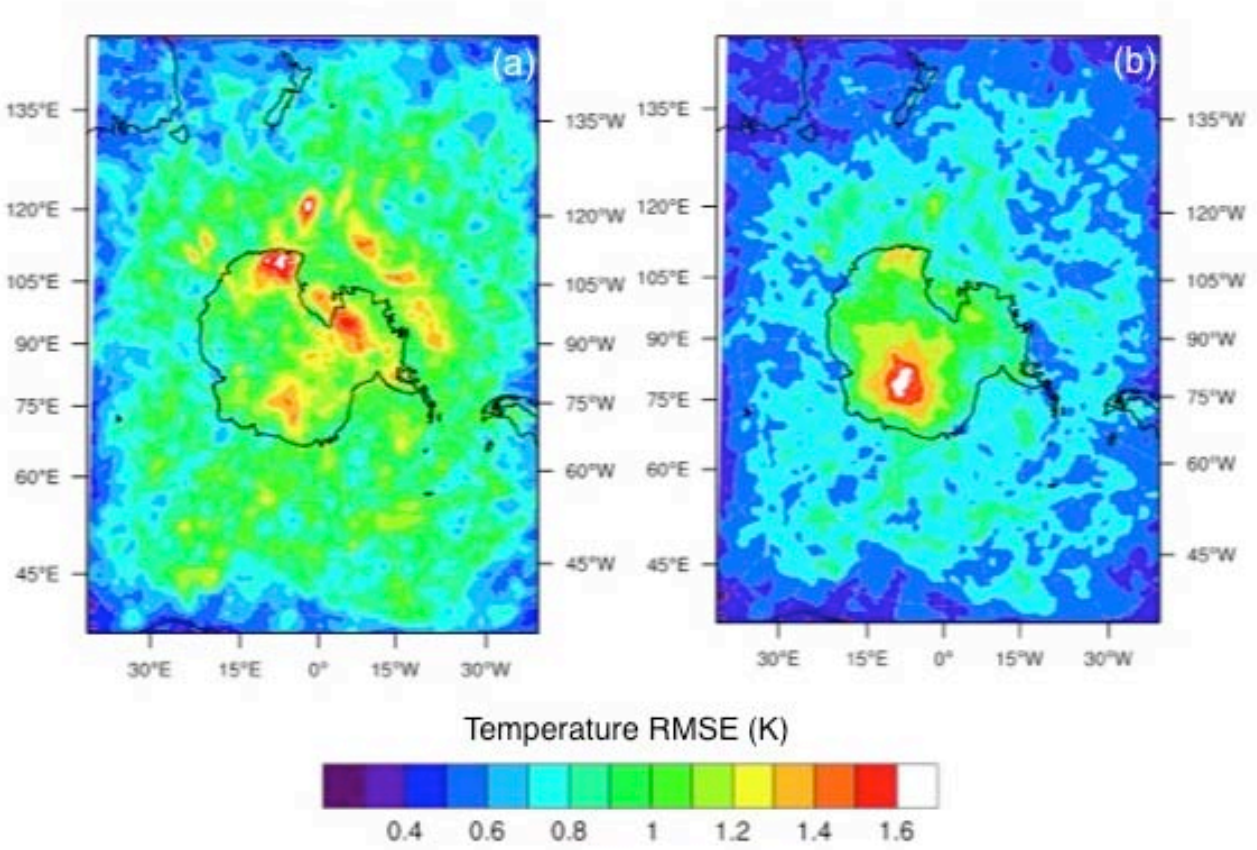

Fig. 10. As in Fig. 7, except the aggregate RMSE of 12-hr forecasts is plotted.

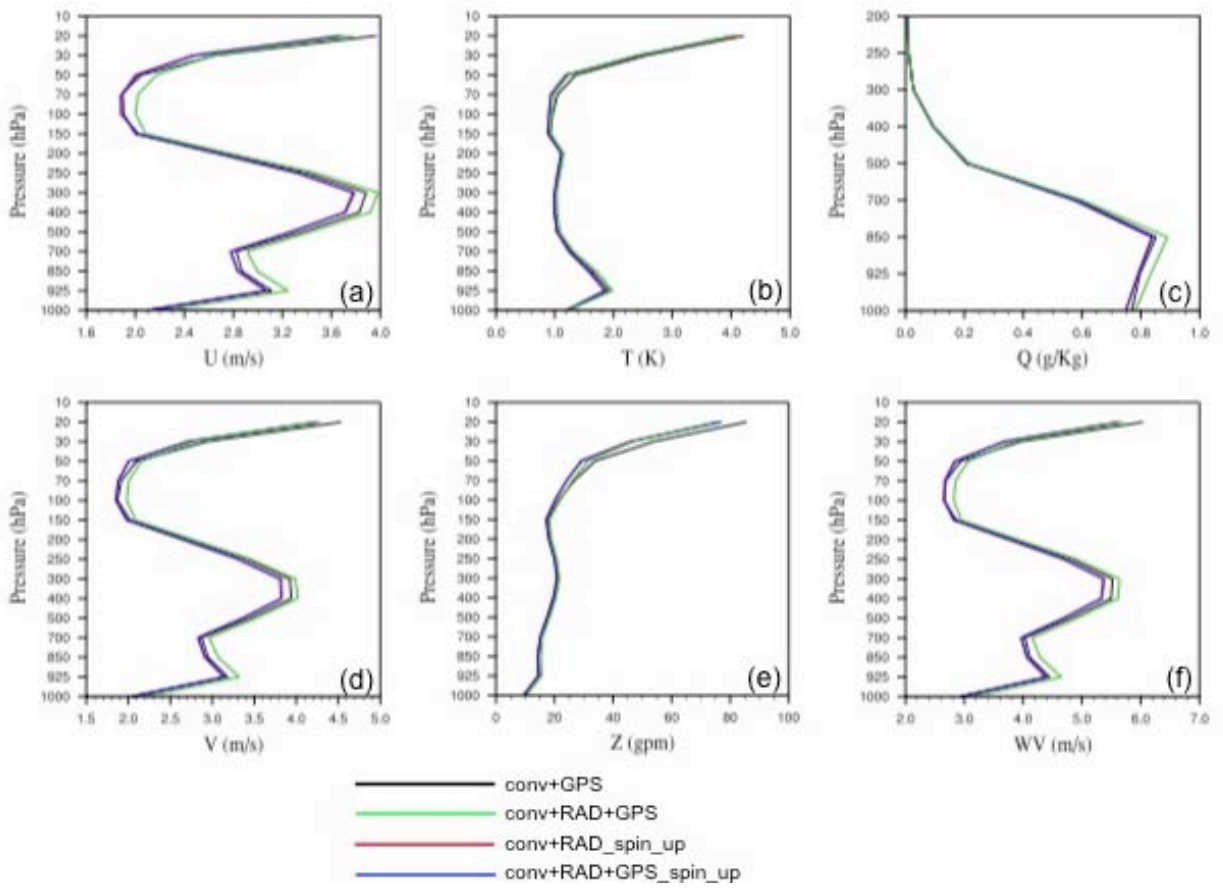

Fig. 11. As in Fig. 5, except the aggregate RMSE of 24-hr forecasts is plotted.

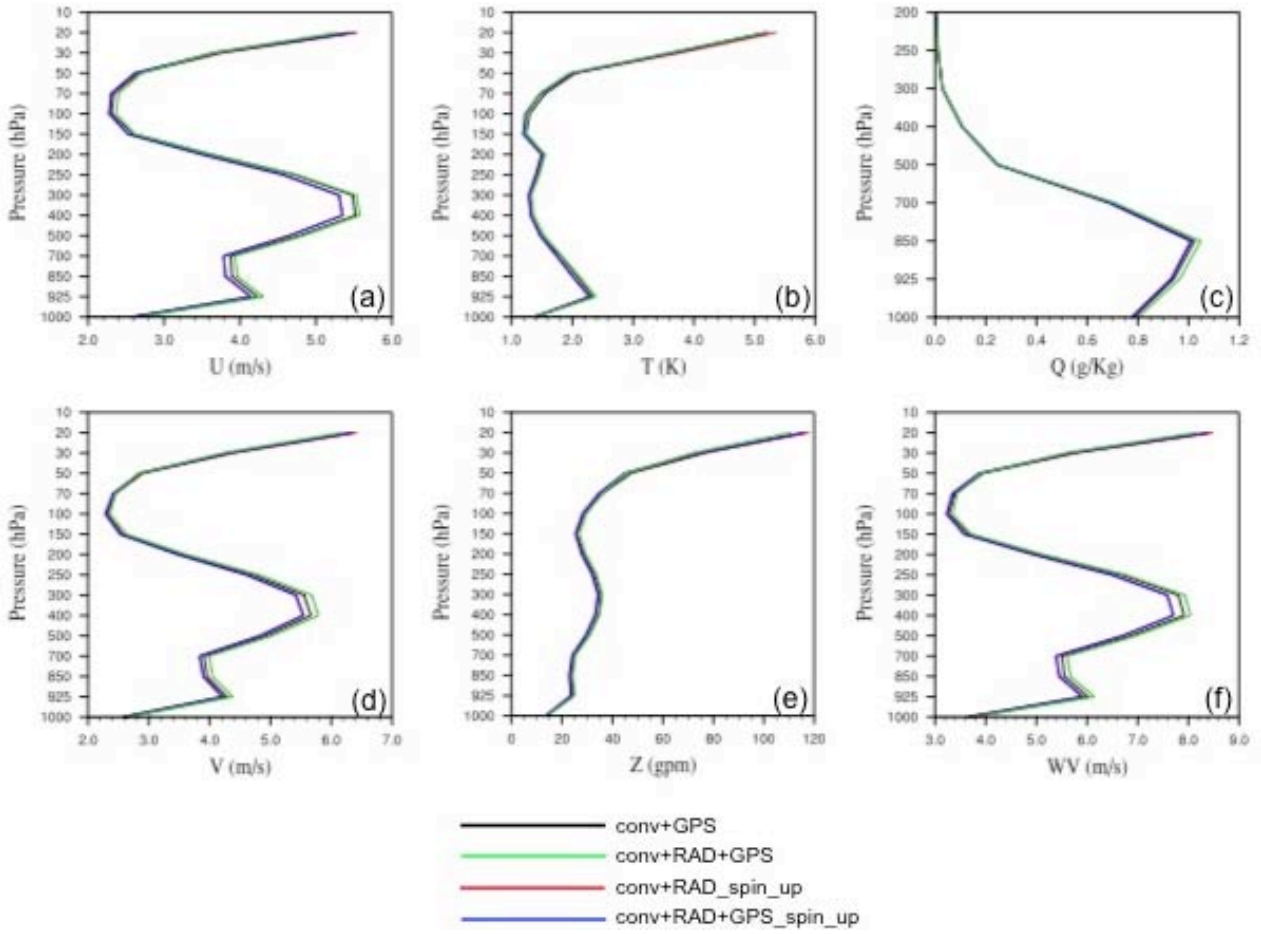

Fig. 12. As in Fig. 5, except the aggregate RMSE of 48-hr forecasts is plotted.